A Comparison between Modeled and Measured ZSU 23-4 at 35 GHz

Tanja Bieker[1], Bert van den Broek[2], Hartmut Schimpf[1]
[1] FGAN-FHR, Neuenahrer Straße 20, D-53343 Werthhoven, Germany
[2] TNO Defense, Security and Safety, Waalsdorperweg 63, 2509 JG The Hague, Netherlands

Introduction

In recent years several powerful RCS modeling codes like Xpatch (US), RAPPORT (NL), Fermat (FR) or FACETS (UK) have been developed. Their medium and long term goal is to replace tower/turntable measurements on real targets.

The advantages of applying RCS modeling codes are many: one does not need the real target, the logistics are much easier, above all, modifications of the target can be accommodated easily, be it the geometry, material properties, or camouflage measures. Thus, all different types of RCS reduction can be implemented and their effects studied.

On the other hand, there are still several shortcomings: it is still not clear which degree of fidelity is necessary for the facet model that describes the target shape. Many different material parameters like dielectric constants and conductivities have to be taken into account. Geometrical imperfectness (angular deviations, surface roughness) has to be considered. The latter becomes the more important the closer the dimensions are to the wavelength.

Due to all these effects the present situation is such that one cannot yet fully trust modeling results when applied to problems like “automatic target recognition” (ATR), especially the training of ATR algorithms. Rather, it is still of great importance to compare the modeling results to real high resolution measurements (e.g. tower / turntable) in order to verify their accuracy or to identify any shortcomings.

For the present analysis, the Dutch RCS modeling code RAPPORT was used on a 600,000 facet model of the ZSU 23-4 air defence tank, provided by ARL /xxxARL/. The computations were performed simultaneously at TNO and at FGAN, the results of different aspect angle intervals combined afterwards.

For comparison, an ISAR tower/turntable measurement of the same target, also performed by ARL was used.

The paper is organized as follows: First, the data that are used will be described in detail, especially the RCS modeling code RAPPORT. Next, several approaches to quantitatively characterize the fidelity of the modeling results will be presented. The main conclusion will be that there is a certain agreement between both data sets, but that even for the high number of facets, the modeling results are not yet fully satisfactory for their use in ATR algorithms.

Description of the data

Tower/turntable data

The radar parameters and measurement geometry were identical in both cases:

- RF frequency 35 GHz
- polarization VV and HH
- bandwidth B=1.5 GHz, achieved by means of frequency agility (256 steps of Δf=5.882 MHz).
- Depression angle 12°
- Angular step $\Delta\alpha$=0.015°, corresponding to 24,000 frequency profiles out of 360° aspect.

Bieker, T.; van den Broek, B.; Schimpf, H. (2005) A Comparison between Modeled and Measured ZSU 23-4 at 35 GHz. In *MMW Advanced Target Recognition and Identification Experiment* (pp. 14-1 – 14-12). Meeting Proceedings RTO-MP-SET-096, Paper 14. Neuilly-sur-Seine, France: RTO. Available from: http://www.rto.nato.int/abstracts.asp.

UNCLASSIFIED/UNLIMITED

Report Documentation Page

Form Approved
OMB No. 0704-0188

1. REPORT DATE **01 MAY 2005**	2. REPORT TYPE **N/A**	3. DATES COVERED **-**
4. TITLE AND SUBTITLE **A Comparison between Modeled and Measured ZSU 23-4 at 35 GHz**		5a. CONTRACT NUMBER 5b. GRANT NUMBER 5c. PROGRAM ELEMENT NUMBER
6. AUTHOR(S)		5d. PROJECT NUMBER 5e. TASK NUMBER 5f. WORK UNIT NUMBER
7. PERFORMING ORGANIZATION NAME(S) AND ADDRESS(ES) **FGAN-FHR, Neuenahrer Straße 20, D-53343 Werthhoven, Germany**		8. PERFORMING ORGANIZATION REPORT NUMBER
9. SPONSORING/MONITORING AGENCY NAME(S) AND ADDRESS(ES)		10. SPONSOR/MONITOR’S ACRONYM(S) 11. SPONSOR/MONITOR’S REPORT NUMBER(S)
12. DISTRIBUTION/AVAILABILITY STATEMENT **Approved for public release, distribution unlimited**		
13. SUPPLEMENTARY NOTES **See also ADM202152., The original document contains color images.**		
14. ABSTRACT		
15. SUBJECT TERMS		

16. SECURITY CLASSIFICATION OF:			17. LIMITATION OF ABSTRACT	18. NUMBER OF PAGES	19a. NAME OF RESPONSIBLE PERSON
a. REPORT **unclassified**	b. ABSTRACT **unclassified**	c. THIS PAGE **unclassified**	**UU**	**37**	

Standard Form 298 (Rev. 8-98)
Prescribed by ANSI Std Z39-18

Range profiles were obtained by means of a 256-point FFT of the frequency profiles. Thus, the unambiguous range $R_E=c/2\cdot\Delta f$ = 25.5meters was subdivided in 256 range cells of size ΔR=0.1m each. ISAR images were obtained by means of a Doppler DFT as described below.

Modeled Data

The simulation program RAPPORT (Radar Signature Analysis and Prediction by Physical Optics and Ray Tracing) has been developed at TNO-FEL in The Netherlands and is based on Geometrical Optics (GO) and Physical Optics (PO). For a detailed introduction of RAPPORT we refer to van den Broek et al. (MATRIX 2005).
For the prediction the same aspect angle and frequency parameters as in the measurement have been used in order to ensure comparability between predicted and measured data.
The prediction has been obtained by FGAN-FHR and TNO. Calculations have been done at FGAN-FHR on a 64-node Linux cluster with 1.3 GHz clock frequency and 1 Gbyte RAM on each processor and at TNO on a single 2Ghz PC using a Linux operating system. Under these conditions the calculation of a single range profile of the 600.000-patches model takes about two minutes at FGAN-FHR and 10 minutes at TNO.

Comparison of measured and modeled data

The question now is how to compare measured and modeled results. Certainly it is important to visually compare images, which provides an intuitive means to judge fidelity. However, this can only be a very first step. More important is: how can a comparison be performed in a quantitative way?
There are essentially three approaches that may be pursued, and which will be described in detail in the following:

1) comparison based on range profiles using high range resolution (HRR). These profiles are obtained by performing a discrete Fourier transform (DFT or FFT) on the frequency profiles that result from the stepped frequency waveform. The comparison can be done using cross correlation coefficients, or by computing some distance measure.
2) Comparison based on ISAR images. These images are obtained by grouping a series of consecutive HRR profiles and performing a “cross-range” DFT within each individual range cell. Again, the quantitative comparison can be done by means of cross correlation or some distance measure.
3) When the main purpose of RCS modeling is the training of ATR algorithms, then the principal issue is to establish the statistics of target recognition features as a function of aspect angle. Feature computation is commonly based either on HRR profiles or on ISAR images. Therefore, an interesting approach is to select a group of features (either specific to the application, or generic), and to compare the feature statistics of modeled and measured data. Here, the Kolmogorov-Smirnow distance measure (KSD) is a powerful tool.

All three methods will be described in some detail in the following.

Comparison based on HRR profiles

Before one can quantitatively compare the range profiles one has to be sure that they are aligned correctly. This alignment has to be performed in range as well as in aspect angle. The difference in range position within the DFT unambiguous range is caused by a different absolute phase term. The angular misalignment is simply caused by the positioning of the target on the turntable which is never as perfect as the "positioning" of the CAD model in the modeling code.

How can these two alignments be achieved?

One starts by plotting all HRR range profiles out of 360° in one diagram (fig.1). This diagram yields a very characteristic pattern which shows "tracks" of all major scattering centers depending on their angular visibility.

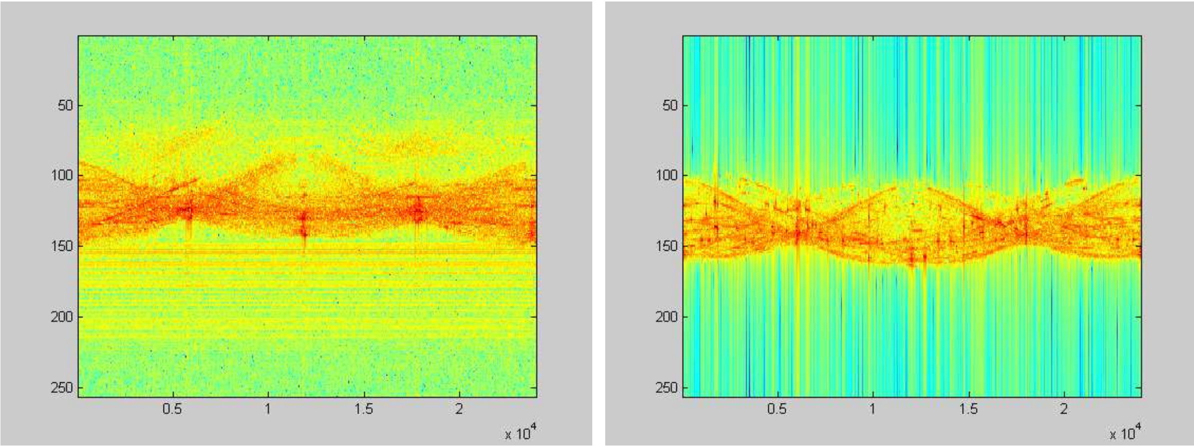

Fig.1 *measured (left) vs. modeled range profiles, HH polarization, viewing direction is from bottom*

A very nicely structured part is seen around 90° (broadside) aspect, around profile #6000. Although one sees that the turntable data appear less structured than the modeled ones, this part can be used for comparison between the two data sets.

As a first approximation it is assumed that there is no angular offset. Then one can form pairs of related range profiles for which the cross correlation coefficient is computed. For a series of profiles n_1 to n_2 one gets the correlation maximum m_c and the related range shift p_r (fig.2).

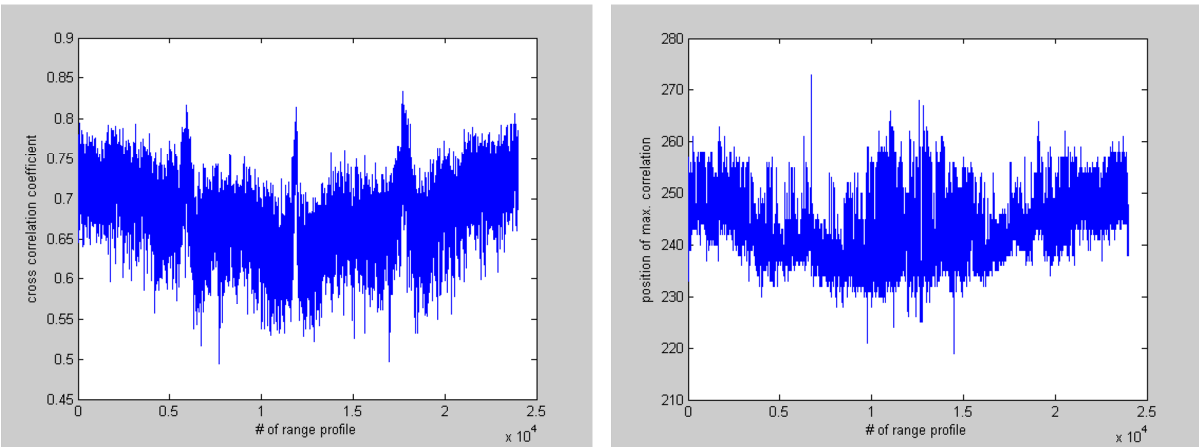

Fig.2 *maximum cross correlation coefficient (left) between modeled and measured HRR profiles and position of maximum*

Those values are not constant but show a certain variation. In order to find the overall range offset one can either use the unweighted mean of p_r or the weighted mean (with the cross correlation coefficient maximum as the weight).

$$\bar{p}_r = \frac{\sum_i p_r(i) \cdot m_c(i)}{\sum_i m_c(i)} \qquad (1)$$

In the first case one gets 242.9, in the second case 243.0 which is in astonishing agreement. As the correlation length is 256 (i.e. the number of range cells after the range FFT) this means a range shift of 13 cells. Stated otherwise, the range intervall 81 to 150 (turntable) corresponds to the intervall 94 to 163 (modeled).

With this offset determined one can now look for a possible angular offset. For this purpose we use again the test area around 90° aspect. As reference, we define an area "test" out of the modeled HH data. We now shift the corresponding test areas against each other and look where

$$d(m,n) = \sum_{i,j} \left\| test_{HH}(i,j) - measured_{HH}(i+m, j+n) \right\| \qquad (2)$$

reaches its minimum. This is the case for a shift of 180 HRR profiles (profile N(turntable) corresponds to (N+180)(modeled) which corresponds to 2.7° angular misalignment of the target on the turntable (fig.3)).

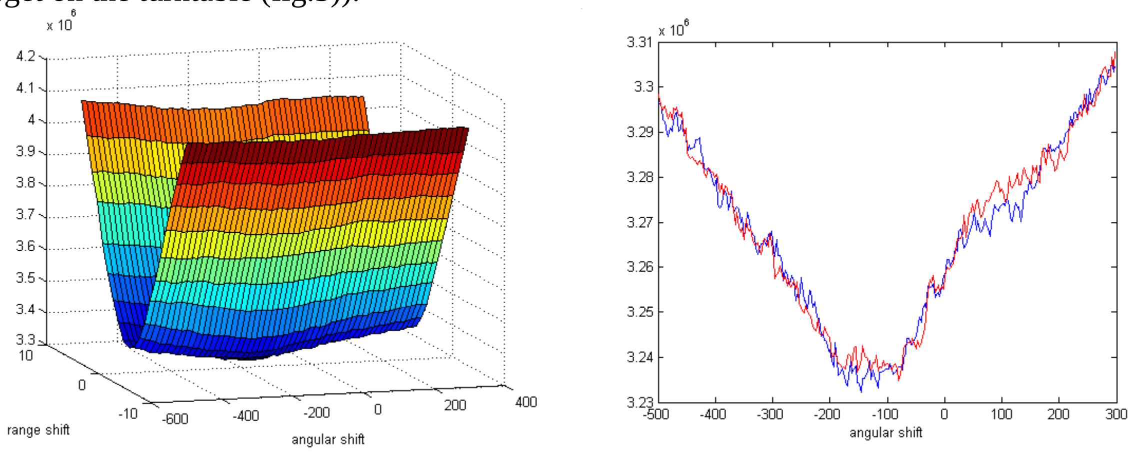

Fig.3 *difference between test area(modeled) and corresponding area (measured), HH and VV(red) show good agreement (right: cut along the "range shift=0" line)*

These are the numbers obtained for the HH data. If one repeats the same analysis for the VV data, one gets an angular offset of only 140 profiles (2.1°). As there is no physical or computational reason for such a difference this difference obviously reflects the error margin of the method. Looking at how shallow the minimum of expression (2) is (fig.3) this seems plausible. For consistency the value of 180 was used for all subsequent analysis.

Comparison based on ISAR images

The angular alignment that was obtained on the basis of HRR profiles also determines which pairs of ISAR images have to be compared to each other. Also, the range alignment has to be applied, of course. However, it turns out that the position of the ISAR image within the Doppler (or cross-range) unambiguous range can be variable. This is due to the special processing of the turntable data: in order to eliminate returns from the surroundings of the platform, and from the platform itself, the "zero Doppler" part of the signals was subtracted before the Doppler DFT was performed. The CAD model, on the other hand, is ideally clutterfree and does not need this kind of processing.

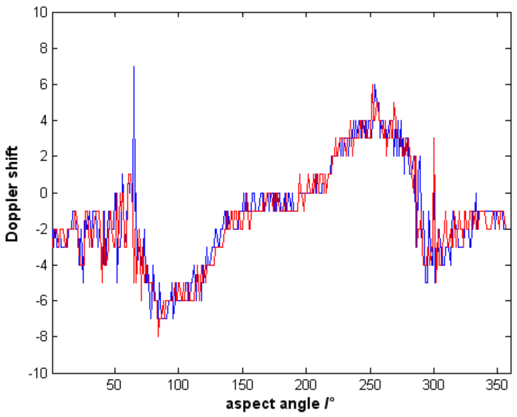

fig.4 *angular minimum of difference between corresponding test areas*

The ISAR processing was performed such that the cross-range resolution equals the range resolution ("square pixels"). The latter is c/2B=0.1m for a bandwidth of 1.5GHz. In order to achieve the same value for the cross-range resolution an aspect angle interval of $\Delta\alpha$=2.46° has to be processed ($\Delta_\perp = \lambda/\Delta\alpha$). This corresponds to roughly 160 profiles, therefore, a 160-point DFT was used for the Doppler processing. In order to obtain one ISAR per 1° aspect, the processing was done in an overlapping manner with a step of 66 profiles from one ISAR image to the next.
Comparing now related pairs of ISAR images (after range and aspect alignment) shows that they still may differ with respect to their Doppler position. Using again the cross correlation coefficient as a function of Doppler shift one finds that this offset is not constant but shows avariation from one ISAR image to the next. This is confirmed by doing the same anylysis for HH and VV: the agreement is extremely good (fig.4). Therefore these offsets are now used to extract congruent ISAR images which are expected to be aligned precisely to the pixel and thus lend themselves for the comparison proper between turntable and modeled ISAR data.

After proper alignment in range, aspect and Doppler the most important comparison is a geometrical one, i.e. looking for the positions of dominant scatterers. For this purpose we eliminate the amplitudes by defining a threshold T=0.8 on the logarithmic (dB) images after rescaling them to the [0 1] interval:
I' = (I – min)/(max – min)
The value T=0.8 turned out to be the optimum one, retaining all dominant scatterers and thus preseving the main structures of the ISAR images. All pixels with I' ≥ T are set to +1, all pixels with I' < T are set to 0 (binary filter). The result are the two segmented ISAR images T (turntable) and M (modeled) as a function of aspect angle. If we now construct a combined image
B = T + 2*M
then this resulting image B has only four different values:

0	:	neither T nor M have a strong scatterer
1	:	only T has a strong scatterer
2	:	only M a strong scatterer
3	:	T and M both have a strong scatterer

An example is given in fig.5 for the aspect 111°.

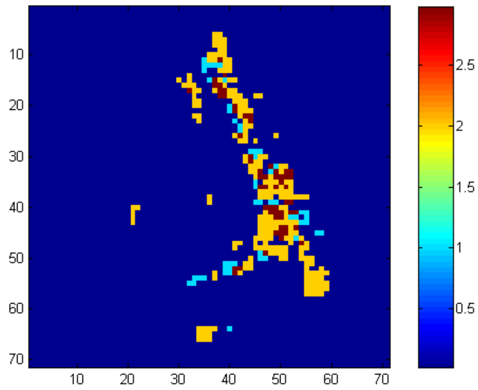

Fig.5 *combined segmented ISAR image B=T+2M*

In order to get an impression of the overall (all 360°) agreement between scatterers it is of interest to look at the fractions of pixels with value 1, 2 or 3 w.r.t. all "filled" pixels (which are not zero and thus show strong scattering). This is shown in fig.6. As one sees, the fraction of common scatterers for HH lies between 5% and 20% with an average of 11.8% whereas for VV the average is slightly higher (12.7%).

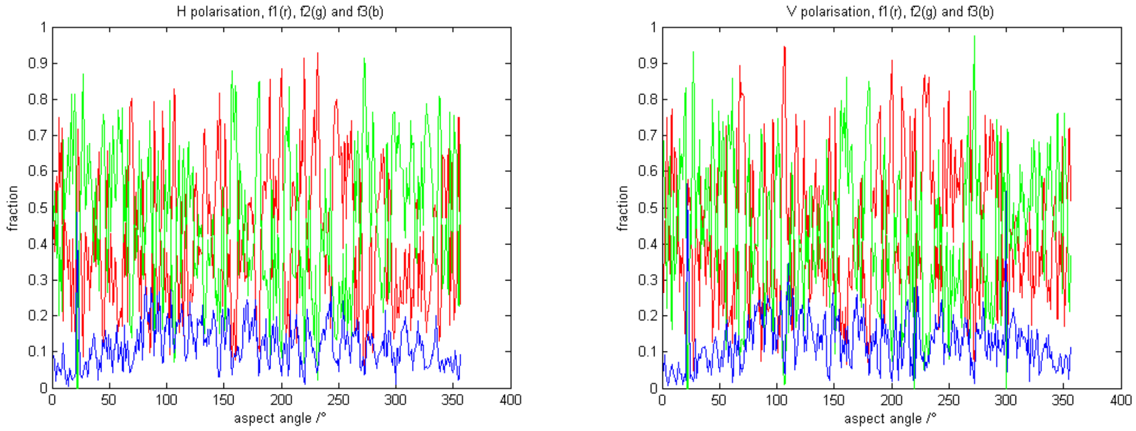

Fig.6 *fractions of scatterers common to modeled and measured ISAR images for HH(left) and VV, f_1=red, f_2=green, f_3=blue*

A more statistical approach to the comparison between correponding pairs of ISAR images is by means of the cross correlation coefficient, taking into account not only position, but also amplitude of the scatterers. Moreover, for the computation of the cross correlation coefficient all pixels of the ISAR images are used, not only the strong ones. The result is shown in fig.7. As one sees, the values do not vary very much over 360°, they are mostly between 0.5 and 0.6. Novak et al. (1994) found that 0.7 is a good value for matching, so that the result is not excellent but reasonable. The front aspect shows the lowest correlation, a maximum occurs around 120°, there is no obvious left/right symmetry. The agreement between HH and VV is excellent.

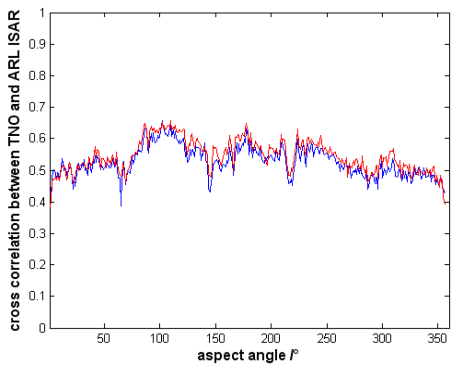

Fig.7 *cross correlation between modeled and measured ISAR images (after alignment)*

Comparison based on feature statistics

For this type of anylysis, the following set of "generic" ATR features was selected:

- ft1 = range extent of 20 strongest scatterers
- ft2 = cross-range extent of 20 strongest scatterers
- ft3 = ft1*ft2 (= area of the "minimum bounding rectangle" (MBR))
- ft4 = mean/std.dev.(total power|MBR)
- ft5 = (powersum 10 strongest scatterers) /powersum(MBR)
- ft6 = log10(pmax(1)/pmax(5)) (ratio between strongest and 5th strongest scatterer within the MBR)
- ft7 = log10(pmax(1)/pmin)|MBR (ratio between strongest and weakest scatterer within the MBR)

which has already been used in former analysis (SPIE xxx) and is extracted from a collection of ATR features (xxx) put together by SET-069. All features were either computed on the HH or on the VV power image. All alignments (range, aspect, Doppler) were taken into account.
As one sees, these features are based on geometry, statistics, and on how the backscatter power is concentrated in more or less predominant scatterers. Due to the immense processing effort which is required at millimetric frequencies, only the "co-polar" return channels (VV and HH) could be modeled, therefore no polarimetric features can be used.
In order to get sufficient data for local probability density functions (pdf's), the spacing between consecutive ISAR images was reduced to .03° yielding about 12,000 ISAR images out of 360°. This is in agreement with former results on angular decorrelation (Toulouse xxx).
Comparison in the feature domain can be mainly done in three ways: 1) comparing pairs of features modeled/measured in scattering plots, 2) computing cross correlation coefficients and 3) comparing feature statistics. All three methods will be described in the following. A possible fourth method, i.e. feeding measured and modeled target into an ATR scheme and analysing their (dis)similarity w.r.t. classification performance, will be left to future work.

Scattering plots

Fig.8 shows four different examples, namely for fetures #2 (geometrical), #4 (statistical), #6 (scatterer structure) and #7 (scatterer dynamic). The example is taken from the aspect angle interval 0° to 15° (500 data pints) for the VV data sets.
For feature #2 there is no recognizable correlation which is quite astonishing, as the cross-range extent – as opposed to the range extent – is not subject to shadowing effects and therefore should provide a realistic description of the target geometry.
The statistical feature #4 shows characteristic "wood worms" that often have a length of less than 10 points, sometimes are much longer. If one looks at the "worms" as they develop as a function of aspect angle, they are usually not connected amongst each other, but there are large jumps from one "worm" to the next.
The scatterer power feature #6 also shows "worms", but in the temporal development there is a continuous evolution so that it actually is only one long "worm" although very erratic in shape.
The "scatterer dynamic range" feature #7 shows the least amount of correlation. This is not astonishing, because the modeled ISAR images are noise and clutter free, their dynamic range is only determined by the DFT/FFT processing. The measured data, on the other hand appear much more "filled in" and smoother.
The HH data sets were also analysed. The behaviour of the features is identical.

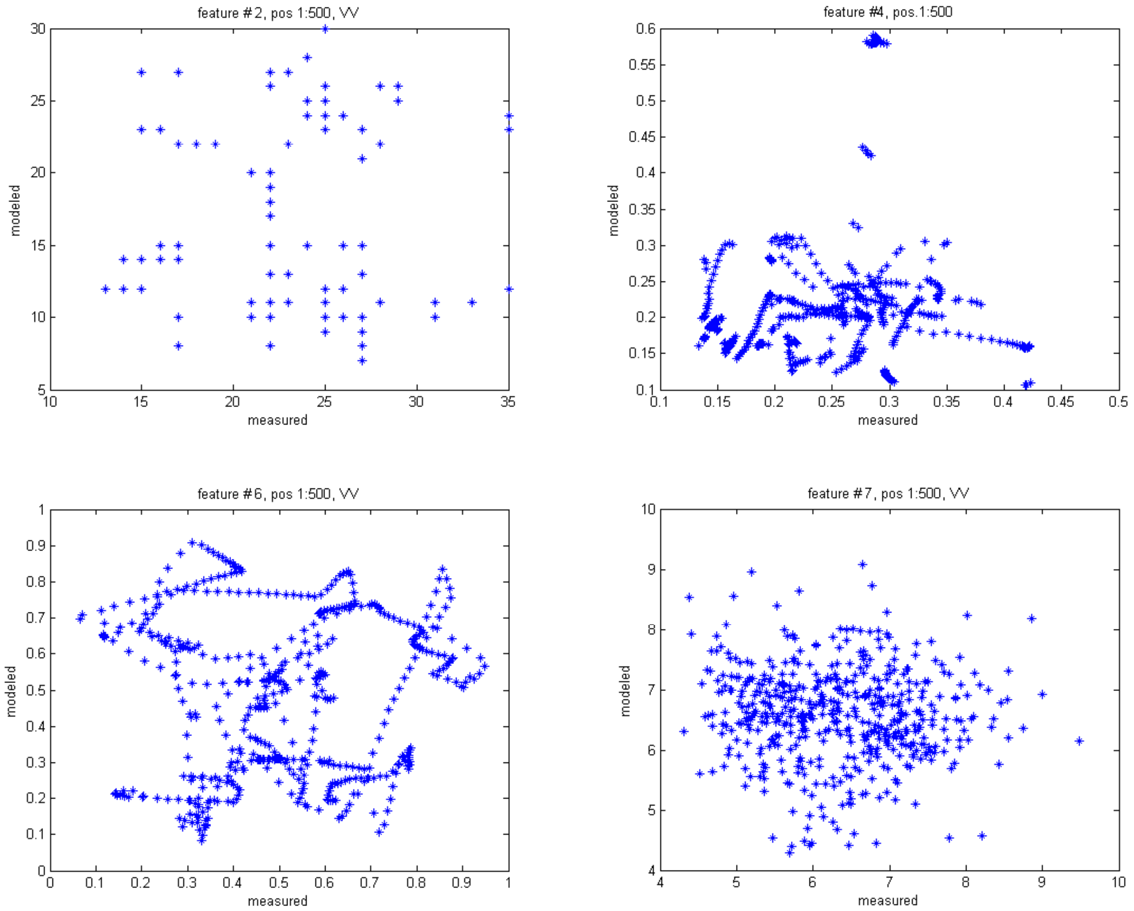

Fig.8 *scatter plots measured vs. modeled data for features2, 4, 6 and 7. Aspect angle 0°-15°, VV polarisation*

Cross correlation coefficient

The cross correlation coefficient ρ is a quantitative way to describe what happens in the scattering plots. It was computed as a function of aspect angle using only a short sliding window of length 100, corresponding to 3°. By definition, ρ can take on values between –1 and +1. As one sees in fig.9 (feature #6) this whole range of values can occur, the fluctuation is considerable.

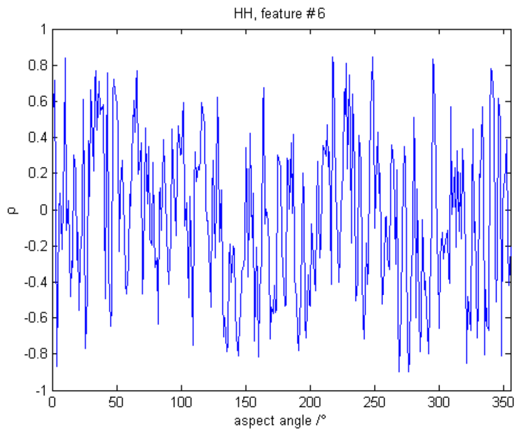

Fig.9 *cross correlation coefficient ρ as a function of aspect angle, ft.#6, HH*

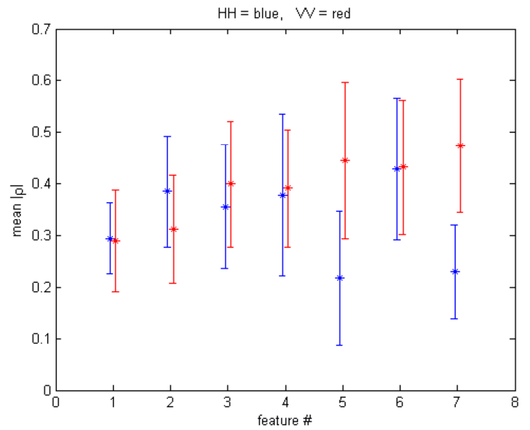

Fig.10 *|ρ| averaged over 360° for all 7 features, HH=blue, VV=red*

If one averages |ρ| over 360° (fig.10) one gets values between 0.3 and 0.5, with rather large standard deviations. The geometric features show less correlation than the scatterer related ones. HH and VV show rather similar behaviour with two exceptions, namely ft.#5 and ft.#7, where ρ(HH) is considerably lower. An explanation for this could not be found.
In general, one can summarize, the correlation between pairs of feature values from measured and modeled data is not very good. Therefore, it seems to be more important to look into local feature pdf's as will be shown in the following paragraph.

Local feature statistics

As ATR performance depends on the aspect angle related feature statistics, it is more important to compare local pdf's than individual feature values. For this purpose, histograms were formed containing 400 values which corresponds to an aspect angle interval of 12°. The angle intervals were chosen with a spacing of 1°.
How can corresponding feature pdf's of modeled and measured data be compared to each other?
A convenient way (Oslo xxx) to compare two pdf's or histograms is by determining the Kolmogoroff-Smirnov distance (KSD) which is defined as the maximum difference between the two corresponding cumulative distributions:
Let $p_1(f)$ and $p_2(f)$ be the two pdf's of a certain feature "f" obtained from the measured and from the modeled data. The respective distribution functions then are

$$P_i(f) = \int_{-\infty}^{f} p_i(f')df' \quad (i=1,2)$$

and hence

$$KS(p_1, p_2) = \max_f |P_1(f) - P_2(f)|.$$

By definition, the KSD can vary between 0 and 1, where "0" means identity, and "1" means complete separation without any overlap.
Now, the KSD was calculated on the basis of the sliding histograms for all 7 features, and for both HH and VV. Three typical examples are shown in fig.11 (fts.2, 4 and 6).

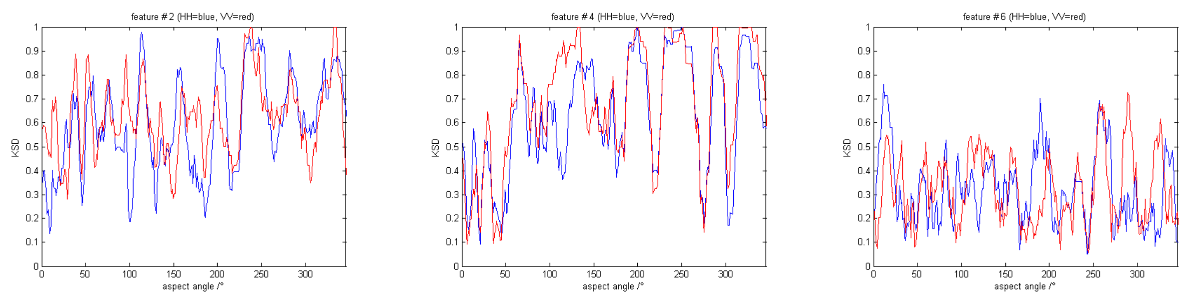

Fig.11 *KS distances between local pdf's of features #2, #4 and #6, HH=blue, VV=red*

In all three examples one sees a strong fluctuation with aspect angle. It does not seem as if the cardinal directions (front, rear and side aspects) play a special role. In many cases, there is a rather similar behaviour for HH and VV. With the exception of feature #6, all KSD curves of HH are strongly correlated to those of VV, with coefficients between 0.64 and even 0.9 (see table below). For ft. #6 there is almost no correlation (0.3).
For similar ATR to be expected, the local pdf's of modeled and measured data should be close to identity, i.e. the pertinent KSDs should be close to 0. As one sees from fts. #2 and 4 (the others are alike) this is by far not the case, with the exception of ft. #6. Very often, even complete separation does occur, whereas the value of zero never appears. The following table

summarizes the diagrams of all 7 features by listing the cross correlation between HH and VV, and the aspect angle averages for KSD(HH) as well as KSD(VV):

feature	*ρ(HH vs.VV)*	*mean-KSD(HH)*	*mean-KSD(VV)*
1	0.67	0.52	0.54
2	0.64	0.59	0.61
3	0.76	0.55	0.605
4	0.86	0.63	0.68
5	0.75	0.47	0.48
6	0.3	0.32	0.32
7	0.9	0.62	0.65

Here again, one sees the special role of feature #6 w.r.t.the others. As one sees, most of the average KSD values lie between 0.5 and 0.65, which means that the pdf's are in rather bad agreement. Therefore it is to be expected that w.r.t. ATR performance studies, the model in its present state is not a good substitute for real measurements.

Summary and Conclusions

Several methods were proposed how to quantitatively compare modeled with measured high resolution turntable data: The HRR profiles were mainly used to perform range and aspect angle alignment. The ISAR images – after aspect angle dependent Doppler alignment, were analysed w.r.t the geometric properties of their strong scatterers (shape, structure). On the average, 12% of all strong scatterers coincide between measured and modeled images. Cross correlation between ISAR images yields values between 0.5 and 0.6 only.

For the analysis of feature statistics 7 generic features of types geometric, statistical, and 'scatterer properties' were introduced. Scatter plots between pairs of features from modeled and measured data show very different behaviour depending on the individual feature. Cross correlation coefficients between 3° intervals of individual features lie between 0.4 and 0.5. Looking into local feature pdf's (12° windows), one finds that the Kolmogorov-Smirnow distance between pdf's from modeled and measured data are mostly above 0.5 which means rather strong dissimilarity.

From all this one can conclude that the similarity between measured and modeled target – using as examples the ARL provided turntable measurements and 600,000 facet model of the ZSU 23-4 – for ATR purposes is not yet satisfactory. In order to rule out the effects of the individual RCS simulation code (RAPPORT from TNO, NL) the same facet model has to be calculated using other codes, too. Results from the French "Fermat" code already exist and will be analysed shortly. Also, US Xpatch results should be made available for comparison.

The main reason for the dissimilarity of the results is expected to be millimeterwave specific effects like surface roughness which are not yet included in present implementations of the codes. The near future will bring considerable improvements in this field.

References

1. **R.J.Chase, Th.M.Kendall, S.R.Thompson**, Parametric Radar Cross-Section Study of a Ground Combat vehicle, SPIE, Orlando, April 2001
2. **NATO-RTO/SET/TG.14 and SET-069 Research and Study Groups**, List of features for Automatic Target Recognition, unpublished
3. **H. Schimpf**, Millimeter Wave ATR - A Study on Feature Robustness, SPIE Proc.**5426** #28, Orlando, April 2004
4. **H.Schimpf, M.Hägelen**, The Influence of Target Aspect Angle Estimation on Robust Target Acquisition, Proc. "Radar 2004", Toulouse, Oct.2004
5. **H. Schimpf**, Robust Acquisition of Relocatable Targets, NATO-RTO SET-080 Symposium on "Target Identification and Recognition using RF Systems, Oslo, Oct.2004
6. **Bert van den Broek, Tanja Bieker, Lucas van Ewijk,** Comparison of modelled to measured high-resolutino ISAR data, Matrix specialist meeting, Oberammergau, May 2005
7. **L.M., Novak, G.J., Owirka, and C.M. Netishen,** Radar Target Identification Using Spatial Matched Filters, Pattern Recognition, Vol. 27, No. 4, pp. 607-617, 1994.

Acknowledgement Our thanks are due to our colleagues from NATO SET-069 Research and Study Group on "Robust Acquisition of Relocatable Targets using Millimeterwave Sensors" for the exchange of high quality data, for the tremendous effort of RCS modeling, and for numerous fruitful discussions and inspiring comments.

A Comparison between modeled and measured ZSU 23-4 at 35 GHz

Tanja Bieker[1], Bert van den Broek[2], Hartmut Schimpf[1]

[1] FGAN-FHR, Neuenahrer Straße 20, D-53343 Werthhoven, Germany
[2] TNO Defense, Security and Safety, Waalsdorperweg 63, 2509 JG The Hgaue, Netherlands

NATO Specialists' Meeting MATRIX 2005
NATO School, Oberammergau, May 10-12, 2005

Overview

- Introduction
- Description of the tower/turntable data
- Description of the modeled data
- Comparison of modeled and measured data
  - Comparison based on HRR profiles
  - Comparison based on ISAR images
  - Comparison based on ATR feature statistics
    - Scattering plots
    - Cross correlation coefficient
    - Local feature statistics
- Summary and conclusions

Introduction

In recent years several powerful RCS modeling codes like Xpatch (US), RAPPORT (NL), Fermat (FR) or FACETS (UK) have been developed. Their medium and long term goal is to replace tower/turntable measurements on real targets.

advantages:

- real target not needed, the logistics are much easier
- modifications of the target can be accommodated easily (geometry, material properties, camouflage measures)
- different types of RCS reduction can be implemented and their effects studied.

shortcomings:

- the degree of fidelity necessary for the facet model that describes the target shape is still not clear
- Many different material parameters like dielectric constants and conductivities have to be taken into account.
- Geometrical imperfectness (angular deviations, surface roughness) has to be considered.

Description of the tower/turntable data

- RF frequency 35 GHz
- polarization VV and HH
- bandwidth B=1.5 GHz, achieved by means of frequency agility (256 steps of Δf=5.882 MHz).
- Depression angle 12°
- Angular step $\Delta\alpha$=0.015°, corresponding to 24,000 frequency profiles out of 360° aspect.

Description of the Modeled Data

- The simulation program RAPPORT (Radar Signature Analysis and Prediction by Physical Optics and Ray Tracing) has been developed at TNO-FEL (NL) and is based on GO and PO.
- the same aspect angle and frequency parameters as in the measurement have been used in order to ensure comparability between predicted and measured data
- Calculations have been done at TNO (single 2Ghz PC, Linux operating system), and at FGAN-FHR (64-node Linux cluster, 1.3 GHz clock frequency, 1 Gbyte RAM on each processor). The calculation of a single range profile of the 600.000-patches model takes about two minutes at FGAN-FHR and 10 minutes at TNO.

High resolution processing

- HRR profiles were obtained by means of a 256-point FFT of the frequency profiles. Thus, the unambiguous range $R_E = c/2 \cdot \Delta f = 25.5$meters was subdivided in 256 range cells of size $\Delta R = 0.1$m each.
- For "square" pixels an aspect angle interval of $\Delta\alpha = 2.46°$ has to be processed ($\Delta_\perp = \lambda/\Delta\alpha$). This corresponds to roughly 160 profiles, therefore, a 160-point DFT was used for the Doppler processing.
- In order to obtain one ISAR per 1° aspect, the processing was done in an overlapping manner with a step size of 66 profiles

Comparison of measured and modeled data

Visually comparing ISAR images provides an intuitive means to judge fidelity. However, more important is: how can a comparison be performed in a **quantitative** way?

- comparison based on HRR range profiles, using cross correlation coefficients, or some distance measure.
- comparison based on ISAR images, using cross correlation coefficients, or some distance measure.
- comparison based on feature statistics, using the Kolmogorov-Smirnow distance measure (KSD)

Comparison based on HRR profiles

- misalignment within the DFT unambiguous range is caused by a different absolute phase term
- angular misalignment is caused by the positioning of the target on the turntable

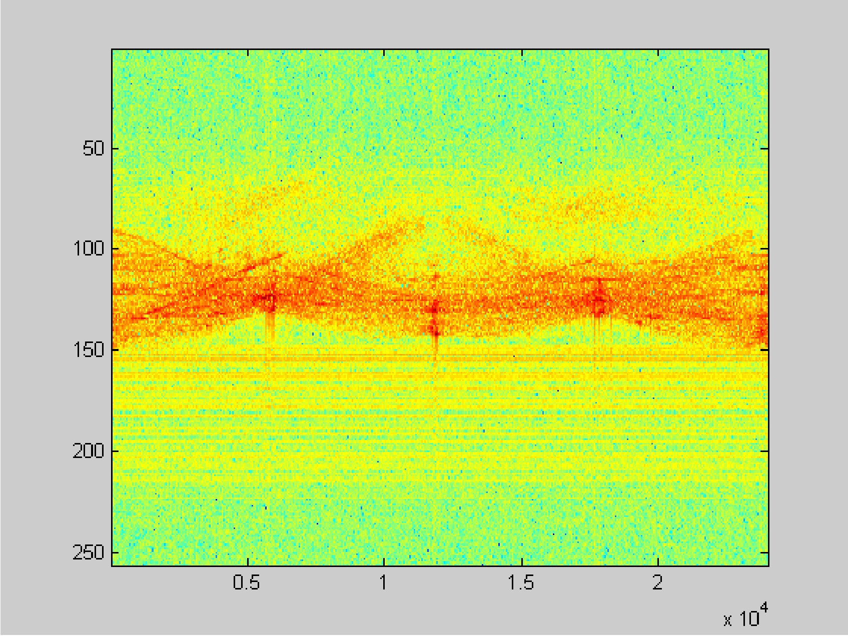

measured

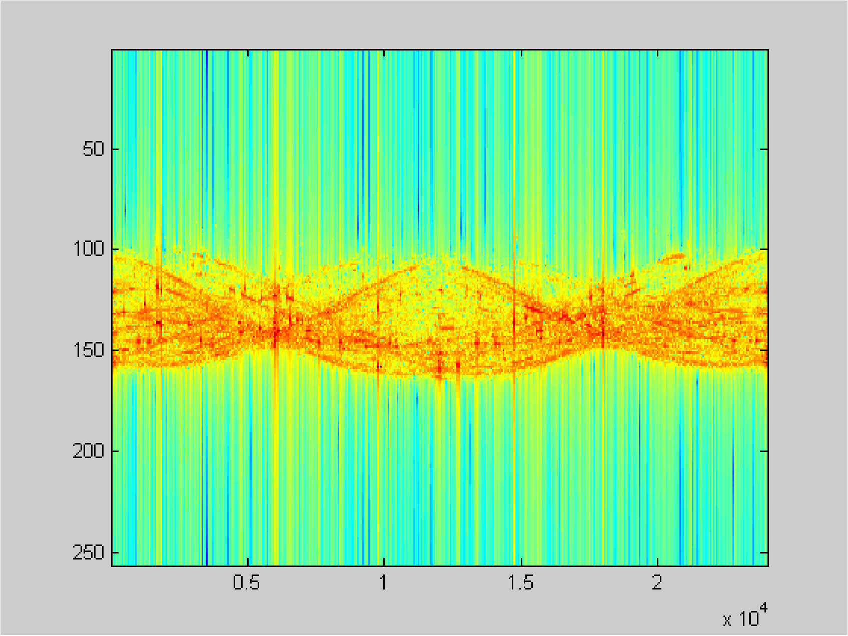

modeled (HH)

Alignment of HRR profiles

- Select a nicely structured part around 90° (profile #6000), corresponding to the right side broadside aspect
- As a first approximation it is assumed that there is no angular offset. Then one can form pairs of related range profiles for which the cross correlation coefficient is computed. For a series of profiles n_1 to n_2 one gets the correlation maximum m_c and the related range shift p_r

Alignment of HRR profiles, cont'd

m_c

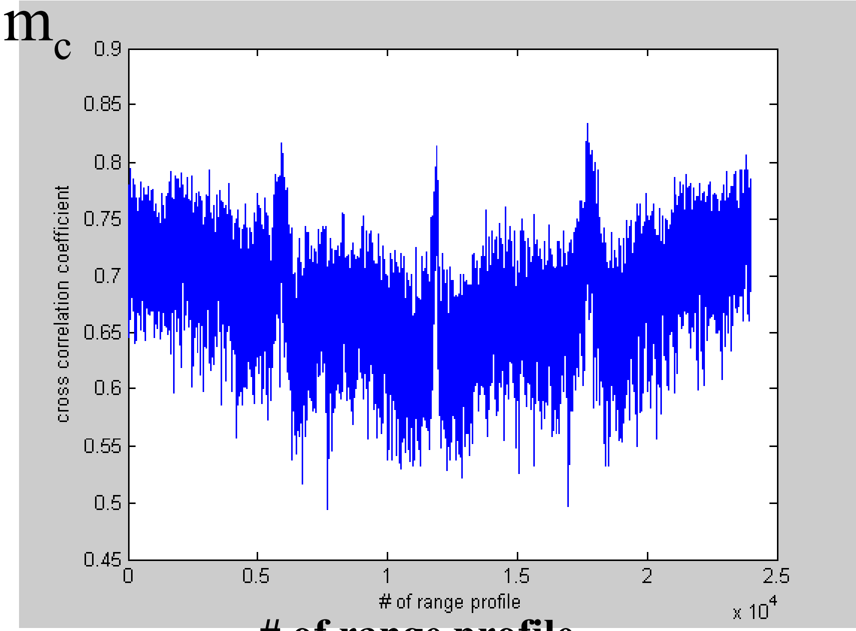

# of range profile

p_r

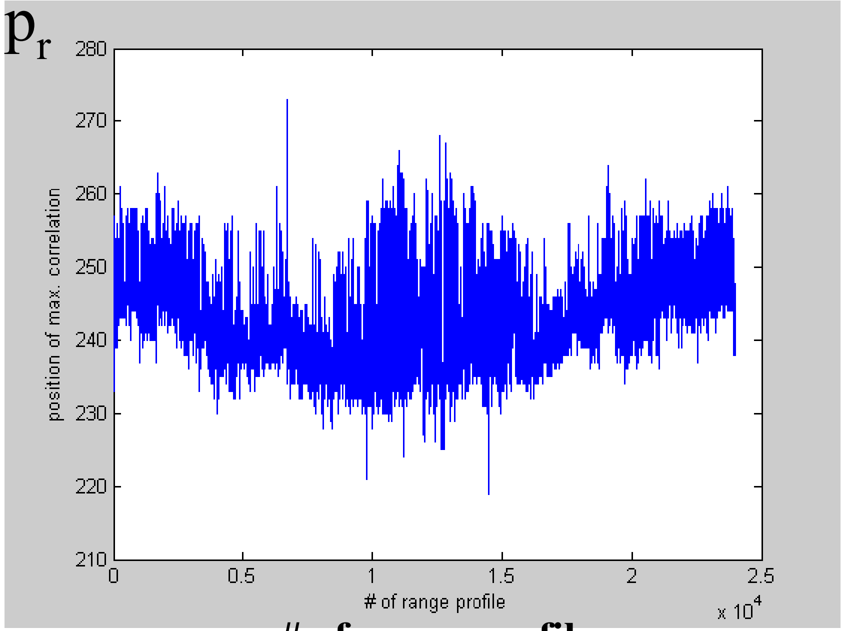

# of range profile

- m_c and p_r are not constant.
- The overall range offset can either can either be computed as the unweighted mean of p_r (242.9) or the weighted mean with the cross correlation coefficient maximum as the weight (243) $\Rightarrow$ shift by 13 range cells: TT(N) $\Leftrightarrow$ modeled(N+13)

Angular alignment

With the range offset determined, we define a reference area "test" out of the **modeled** HH data.
⇒ shift the corresponding test areas against each other and look where

$$d(m,n) = \sum_{i,j} \left\| test_{HH}(i,j) - measured_{HH}(i+m, j+n) \right\|$$

reaches its **minimum**. This is the case for a shift of 180 HRR profiles (profile N(turntable) corresponds to (N+180)(modeled) which corresponds to 2.7° angular misalignment of the target on the turntable

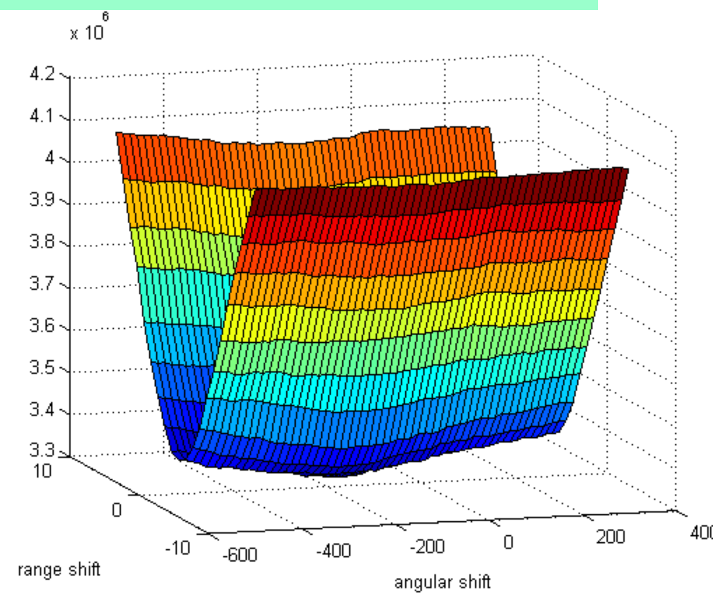

Angular alignment, cont‘d

These are the numbers obtained for the HH data. If one repeats the same analysis for the VV data, one gets an angular offset of only 140 profiles (2.1°).
As there is no physical or computational reason for such a difference this difference obviously reflects the error margin of the method. Looking at how shallow the minimum of expression this seems plausible. For consistency the value of 180 was used for all subsequent analysis.

Comparison based on ISAR images

- The angular alignment determines which pairs of ISAR images have to be compared to each other.
- Also, the range alignment has to be applied.
- The position of the ISAR image within the Doppler (or cross-range) unambiguous range can be variable. This is due to the subtraction of the “zero Doppler” within the turntable data in order to eliminate returns from the platform and its surroundings. The CAD model, on the other hand, is ideally clutterfree and does not need this kind of processing.

Doppler alignment

Using the cross correlation coefficient as a function of Doppler shift shows that this offset is not constant but shows avariation from one ISAR image to the next.
This is confirmed by doing the same anylysis for HH and VV: the agreement is extremely good.
These offsets are now used to extract congruent ISAR images which are expected to be aligned precisely to the pixel

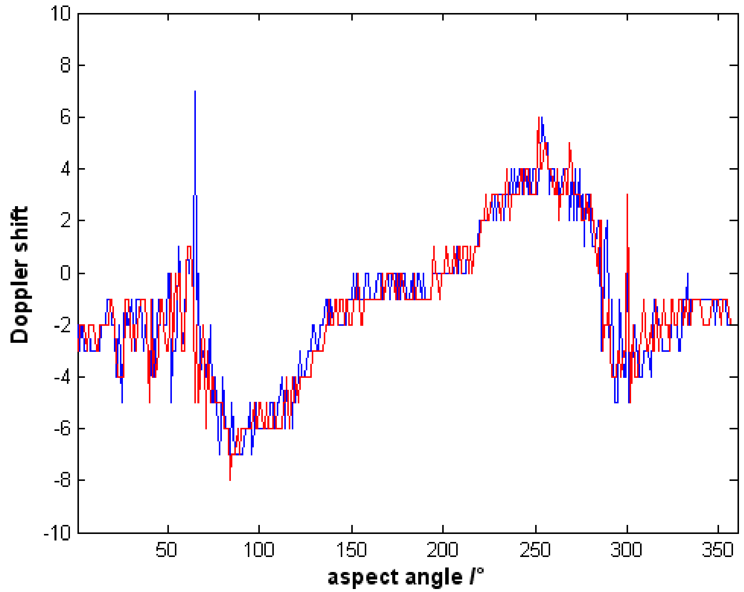

HH (blue), VV(red)

Geometrical comparison of ISAR images

After proper alignment in range, aspect and Doppler eliminate the amplitudes by defining a threshold **T=0.8** on the logarithmic (dB) images after rescaling them to the [0 1] interval:

$$\mathbf{I' = (I - min)/(max - min)}$$

All pixels with I' ≥ T are set to +1, all pixels with I' < T are set to 0 (binary filter). We define a combined image

$$\mathbf{B = T + 2*M}$$

0 : neither T nor M have a strong scatterer
1 : only T has a strong scatterer
2 : only M a strong scatterer
3 : T and M both have a strong scatterer

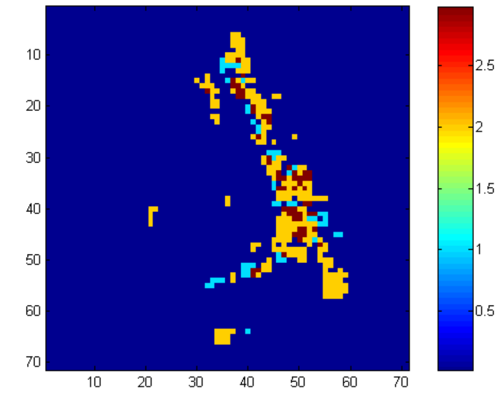

aspect 111°

Common scatterers

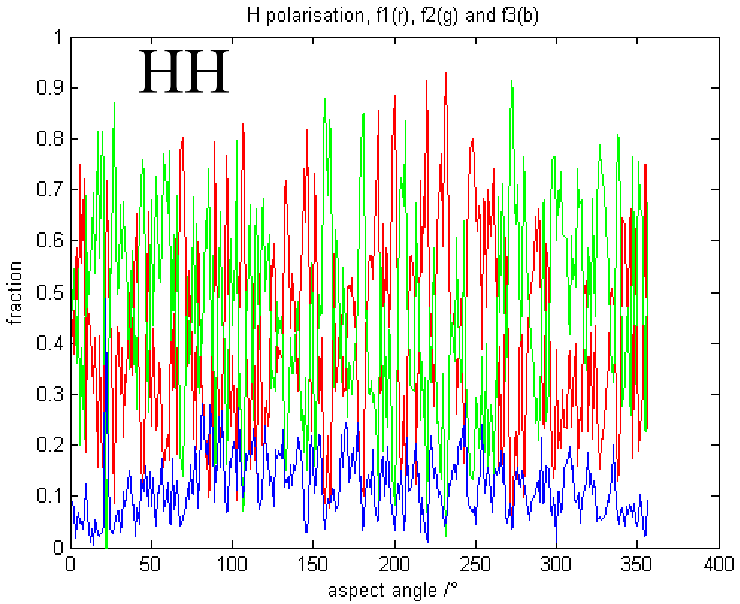

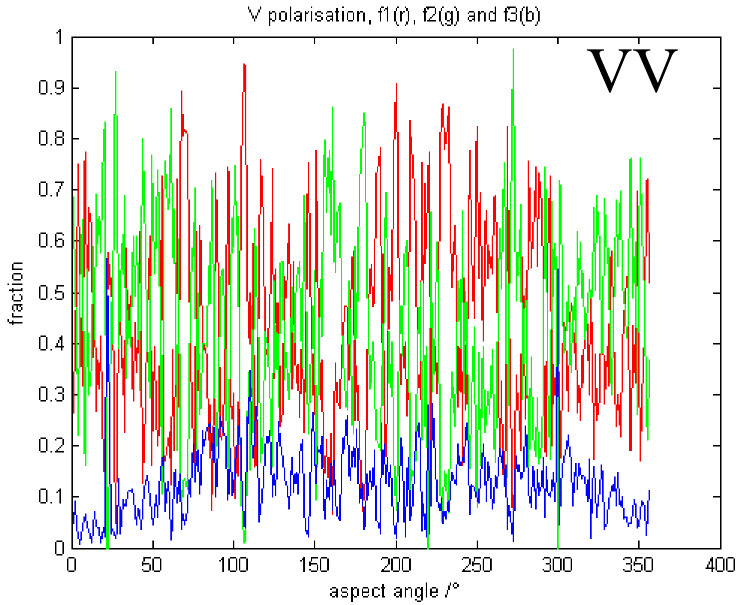

f_1=red, f_2=green, f_3=blue

The fraction of common scatterers (**f_3**) for HH lies between 5% and 20% with an average of 11.8% whereas for VV the average is slightly higher (12.7%).

Cross correlation coefficient

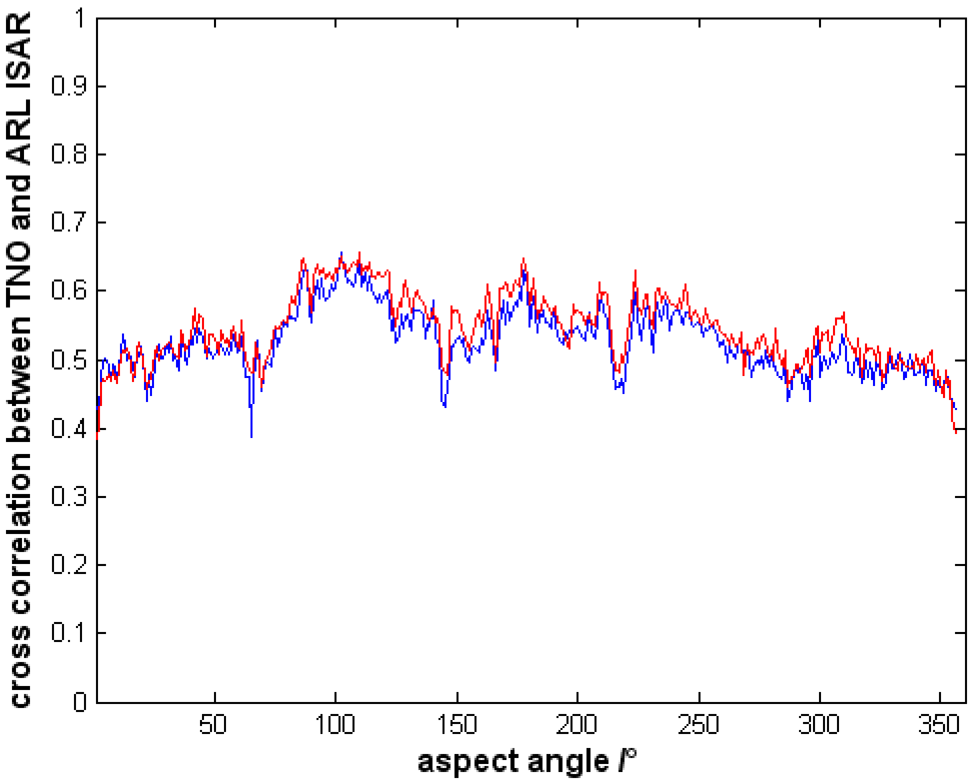

HH (blue), VV(red)

The cross correlation coefficient, takes into account not only the **position**, but also the **amplitude** of the scatterers. Values are mostly between 0.5 and 0.6. Novak et al. (1994) found that 0.7 is a good value for matching, so that the result is not excellent but reasonable

Comparison based on feature statistics

The following set of “generic” ATR features was selected:

- ft1 = range extent of 20 strongest scatterers
- ft2 = cross-range extent of 20 strongest scatterers
- ft3 = ft1*ft2 (= area of the “minimum bounding rectangle” (MBR))
- ft4 = mean/std.dev.(total power|MBR)
- ft5 = (powersum 10 strongest scatterers) /powersum(MBR)
- ft6 = log10(pmax(1)/pmax(5)) (ratio between strongest and 5th strongest scatterer within the MBR)
- ft7 = log10(pmax(1)/pmin)|MBR (ratio between strongest and weakest scatterer within the MBR)

In order to get sufficient data for local probability density functions (pdf’s), the spacing between consecutive ISAR images was reduced to .03° yielding about 12,000 ISAR images out of 360°.

Scattering plots modeled vs. measured

VV 0° - 15°

Ft.2

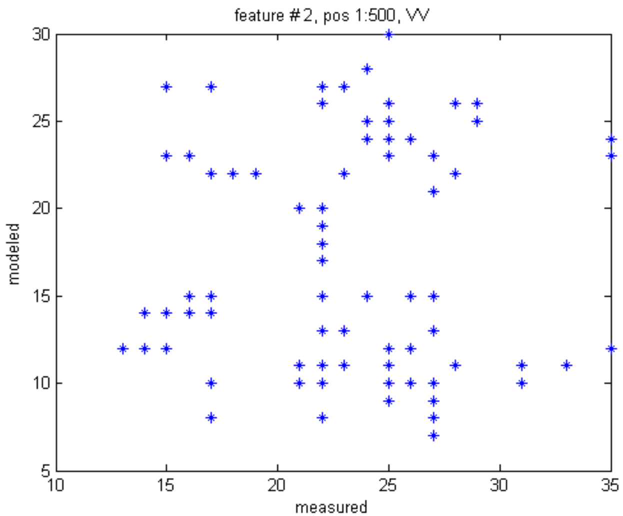

Ft.4

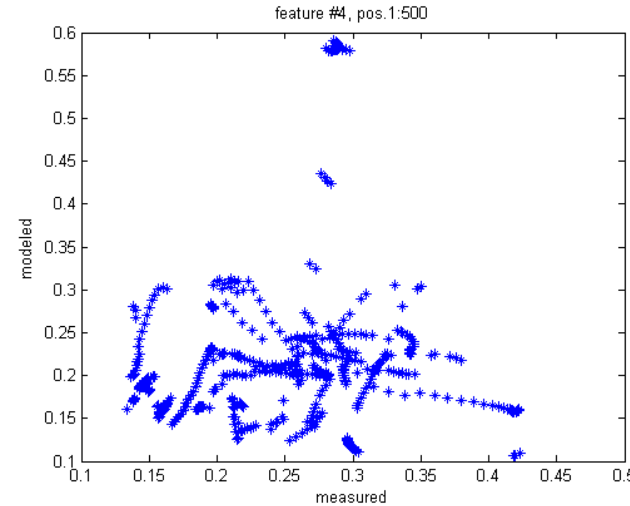

Ft.6

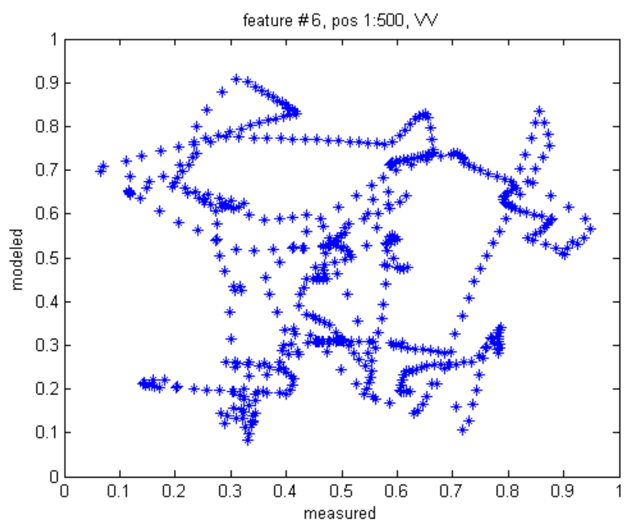

Ft.7

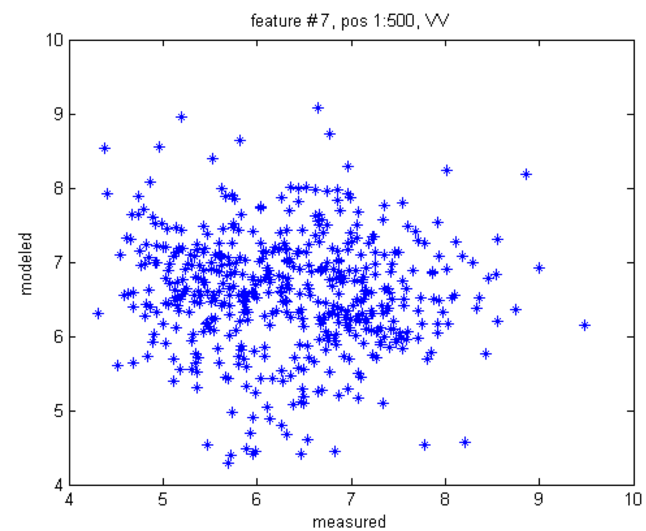

Cross correlation coefficient ρ between measured and modeled data

ρ is a quantitative means to describe the scattering plots.
It was computed as a function of aspect angle using only a short sliding window of length 100, corresponding to 3°.

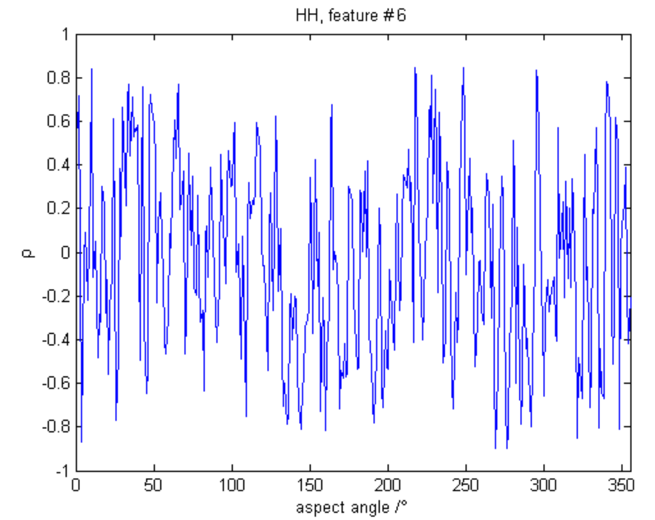

Ft.6, HH

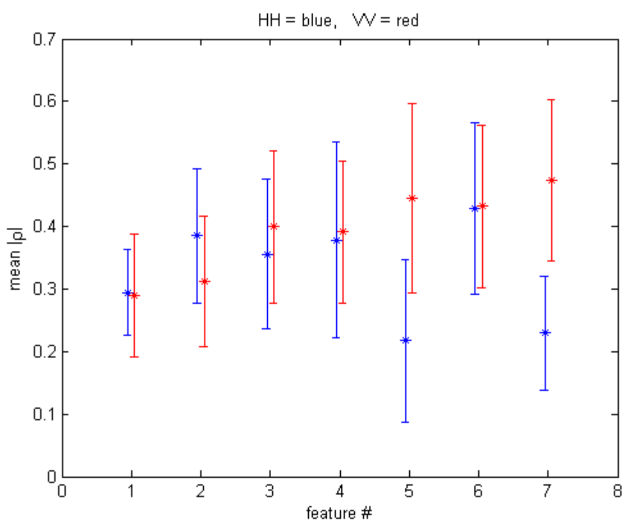

|ρ| averaged over 360° for all 7 features, HH=blue, VV=red

Local feature statistics

- As ATR performance depends on the aspect angle related feature statistics, it is more important to compare local pdf's than individual feature values.
- Histograms were formed containing 400 values which corresponds to an aspect angle interval of 12°.
- The angle intervals were chosen with a spacing of 1°.

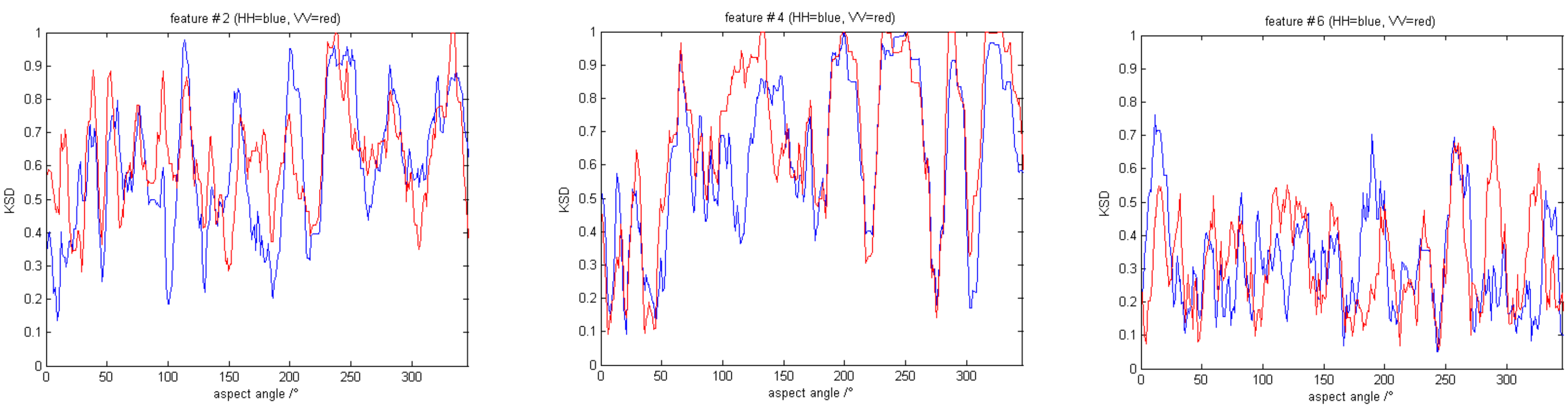

KS distances between local pdf's of features #2, #4 and #6, HH=blue, VV=red

ISAR comparison, summary

feature	*p(HH vs. VV)*	*mean-KSD(HH)*	*mean-KSD(VV)*
1	0.67	0.52	0.54
2	0.64	0.59	0.61
3	0.76	0.55	0.605
4	0.86	0.63	0.68
5	0.75	0.47	0.48
6	0.3	0.32	0.32
7	0.9	0.62	0.65

Feature #6 behaves different w.r.t.the others.
Most of the average KSD values lie between 0.5 and 0.65, which means that the pdf's are in rather bad agreement.
It is to be expected that w.r.t. ATR performance studies, the model in its present state is not a good substitute for real measurements.

Summary and conclusions

- Several methods were proposed how to **quantitatively** compare modeled with measured high resolution turntable data: The HRR profiles were mainly used to perform range and aspect angle alignment.
- The ISAR images – after aspect angle dependent Doppler alignment, were analysed w.r.t the geometric properties of their strong scatterers (shape, structure). On the average, 12% of all strong scatterers coincide between measured and modeled images.
- Cross correlation between ISAR images yields values between 0.5 and 0.6

Summary and conclusions, cont‘d

Analysis of feature statistics:

- 7 generic features of types geometric, statistical, and ‘scatterer properties’ were used for analysis.
- Scatter plots between pairs of features from modeled and measured data show very different behaviour depending on the individual feature.
- Cross correlation coefficients between 3° intervals of individual features lie between 0.4 and 0.5.
- The Kolmogorov-Smirnow distance between local feature pdf’s from modeled and measured data (12° windows) are mostly above 0.5 which means rather strong dissimilarity.

Summary and conclusions, cont‘d

Conclusions:

- The similarity between measured and modeled target – using as examples the ARL provided turntable measurements and 600,000 facet model of the ZSU 23-4 – for ATR purposes is **not yet satisfactory**.
- In order to rule out the effects of the individual RCS simulation code (RAPPORT from TNO, NL) the same facet model has to be calculated using other codes, too.
- Results from the French "Fermat" code already exist and will be analysed shortly. Also, US Xpatch results should be made available for comparison.
- The main reason for the dissimilarity of the results is expected to be millimeterwave specific effects like surface roughness